ORIGINAL RESEARCH

Ultrasound Sonography to Detect Focal Osteoporotic Jawbone Marrow Defects: Clinical Comparative Study with Corresponding Hounsfield Units and RANTES/CCL5 Expression

Johann Lechner [iD] [1]
Bernd Zimmermann [2]
Marlene Schmidt [iD] [3]
Volker von Baehr [4]

[1]Department of Clinical Research, Clinic Integrative Dentistry, Munich, Germany; [2]Medical Devices, QINNO, Wessling, Germany; [3]Department of Statistics, STEYR Motorenwerke, Steyr, Austria; [4]Department of Immunology and Allergology, Institute for Medical Diagnostics Berlin, Germany

Introduction: The presently used impulse echo ultrasound examination is not suitable to provide relevant and reliable information about the jawbone, because ultrasound (US) almost completely reflects from the hard cortical jawbone. At the same time, "focal osteoporotic bone marrow defects" (BoneMarrowDefects = BMD) in jawbone are the subject of scientific presentations and discussions.

Purpose: Can a newly developed trans-alveolar ultrasonic sonography (TAU-n) device locate and ascertain BMD?

Patients and Methods: TAU-n consists of a two-part handpiece with an extraoral ultrasound transmitter and an intraoral ultrasound receiver. The TAU-n computer display shows the different jawbone densities with corresponding colour coding. The changes in jawbone density are also displayed numerically. The validation of TAU-n readings: A usual ortho-pantomogram (2D-OPG) on its own is not suitable for unequivocally determining jawbone density and has to be excluded from this validation. For validation, a 3D-digital volume tomogram/cone beam computer tomogram (DVT/CBCT) with the capacity to measure Hounsfield units (HU) and a TAU-n are used to determine the presence of preoperative BMD in 82 patient cases. Postoperatively, histology samples and multiplex analysis of RANTES/CCL5 (R/C) expression derived from surgically cleaned BMD areas are evaluated.

Results: In all 82 bone samples, DVT-HU, TAU-n values and R/C expressions show the presence of BMD with chronic inflammatory character. However, five histology samples showed no evidence of BMD. All four evaluation criteria (DVT-HU, TAU-n, R/C, histology) confirm the presence of BMD in each of the 82 samples.

Conclusion: The TAU-n method almost completely matches the diagnostic reliability of the other methods. The newly developed TAU-n scanner is a reliable and radiation-free option to detect BMD.

Keywords: trans-alveolar ultrasonography, cone beam computed tomography, RANTES/CCL5, Hounsfield units, cavitational osteonecrosis of jawbone

Introduction

In medicine, impulse echo ultrasound is generally used for all kinds of tissue imaging. In principle, body structure images are generated by analyzing the reflection of ultrasound waves. In a recent systematic review and meta-analysis, the possible use of ultrasonography for evaluating masseter muscles in orthodontic or functional orthopedic treatment was published.[1] However, this method is not suitable to provide

Correspondence: Johann Lechner
Tel +49-89-6970129
Fax +49-89-6925830
Email drlechner@aol.com

medically relevant information about the status of jawbone, because ultrasound is almost completely reflected at the border between bone and soft tissue. In particular, the cancellous part of the jawbone cannot be examined with a commonly used ultrasound. Therefore, ultrasound is only of limited use in dentistry despite "focal osteoporotic bone marrow defects (BMD)" being the subject of scientific papers and discussion.[2,3] Why is their detection necessary for dentists and doctors alike? The condition of the cancellous jawbone can be of great clinical importance. Bouquot has proven that cancellous bone can be largely degenerated. A phenomenon he calls "aseptic ischemic osteonecrosis of jawbone" (AIOJ), which leads to "cavitations". He relates this osteonecrosis of the jawbone to neuralgic pain and defines a disease called "neuralgia inducing cavitation osteonecrosis (NICO)."[4] For the first time, the authors recommend the use of an ultrasound device[5] to detect these lesions. With respect to the conspicuous morphology, we proposed the term "fatty-degenerative osteonecrosis/osteolysis of jawbone" (FDOJ) for this cavitational osteonecrosis,[6,7] additionally to the term of AIOJ. According to publications by AI-Nawas, the status of the cancellous jawbone is of utmost importance for the success of dental implants.[8,9] A major problem, however, is that jawbone with BMD/AIOJ/FDOJ often appears without abnormal findings in x-rays.[10]

Objectives and Questions

This paper presents the latest diagnostic possibilities to measure jawbone density with a new device used in dentistry for trans-alveolar ultrasound sonography (TAU). The new equipment TAU-n calls for clarification whether the measured TAU-n values are reliable and if they correctly reflect clinical states of focal bone marrow defects (AIOJ/BMD/FDOJ). Is TAU-n outcome prediction performance enough?

Materials and Methods
A New Trans-Alveolar Ultrasonography Device

To overcome the previously mentioned challenges, a different approach was necessary. Using innovative trans-alveolar ultrasonic pulses (TAU), the newly developed TAU-n is capable of detecting and locating these cavitations up to the fatty-degenerative dissolution of the medullary trabecular structures in jawbone. The TAU-n device generates an ultrasonic pulse and guides the pulse through the entire jawbone. The pulse is then recorded and measured by an ultrasound receiver. This pulse is generated by an extraoral transmitter

and detected and measured by a receiving unit positioned intraorally. Both parts (ie transmitter and receiver) are parallel fixed in a single handpiece. The size of the TAU-n receiver unit is designed for easy insertion into the patient's mouth. The jawbone must be positioned between the two parts of the measuring unit. The acoustic coupling between transmitter and receiver and the alveolar ridge is achieved using a semi-solid gel. The contact between the extraoral transmitter and the intraoral receiver (Figure 1) is optimized by the use of a special ultrasound gel pad specially developed for this purpose. The results are displayed on a color screen, which shows different colors depending on the degree of attenuation of the ultrasound pulse. Attenuation of the pulse amplitude indicates pathological changes in the jawbone. Each organ and each organ structure show a highly individual attenuation behavior depending on its physiological state. Corresponding values are based on the published data by Wells[11] and Njeh.[12] They are only guiding values due to biological fluctuation.

Display of TAU-n

The TAU-n display can detect the following physical structures in the dentoalveolar and maxillary sinus region, with corresponding color codes from 91 color columns per cm2. Figure 2 assigns the coloring of TAU-n in a left lower jaw area (area 37, 38 and 39/European coding).

- Green or white/light blue = extremely dense and hard structures such as teeth, implants and crowns; solid bone in marginal cortical region; = healthy medullar spongial bone; air components in oral and maxillary sinuses
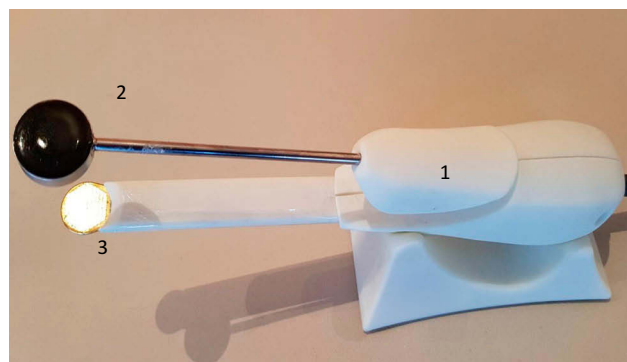- Yellow/blue = fatty nerve structures

Figure 1 (1) Handpiece with ultrasonic transmitter and receiver unit. (2) Ultrasonic transmitter, (3) Ultrasonic receiver with coplanar and fixed arrangement of transmitter and receiver.
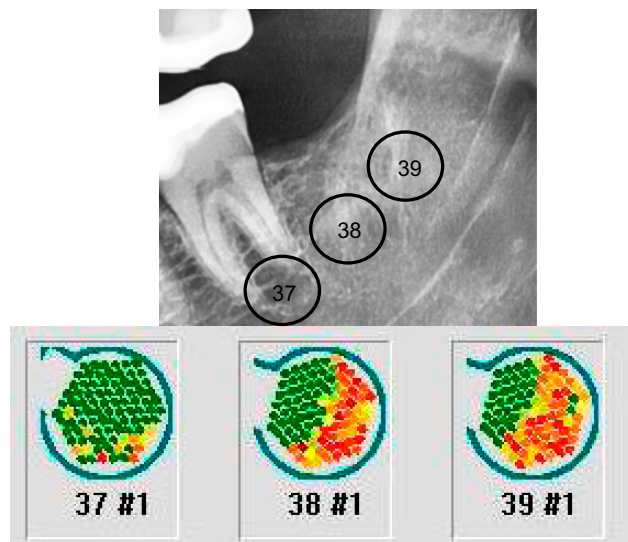
Figure 2 Example of 2D coloring in TAU-n in area 37 = GREEN = solid bone. Area 38 = RED = reduced bone density = fatty-degenerative parts. Retromolar area 39 = RED= decreased bone density = fatty-degenerative parts.

- Red or black/dark blue = chronically inflammatory medullary-spongial bone with fatty-degenerative components

Numerical Bone Density Determination with TAU-n

The TAU-n software numerically displays the attenuation coefficients of the TAU-n measuring range. By clicking on one of the 91 sensor fields the software marks the field and displays the measured value in a logarithmic evaluation. The cells to be evaluated are selected and highlighted with a mouse click. The display shows the number of marked cells, the resulting mean value and the corresponding color. TAU-n calculates the logarithmic mean value of the sum of the lowest sensor elements as "mean value (log)" in RED. The logarithmic mean value of the highest sensor elements is also displayed in GREEN – corresponding to the reduced attenuation by a fixed structure (see Figures 3, 4 and 5).

The TAU-n software thus allows the mean value to be calculated over a freely selectable cell range of the 91 piezoelectric sensors. The averaging is logarithmic: The meaning of logarithmic averaging is that the color change to green already occurs at relatively small values (eg 3); however, the value range goes up to a total of 100. This means that green fields are much more important than red fields with linear averaging. Example: A green field with value 100 and 10 red fields with value 1 are marked. The linear average results in $(100 + 10*1)/11 = 10$, which averages the colour green. With logarithmic averaging, the logarithms of the values are averaged and the exponential value shown: $\log10(100) = 2$, $\log10(1) = 0$ would be the average value of the logarithms $(2 + 10*0)/11 = 0.18$. The exponential value is then $10^{0.18} = 1.52$. This would show red to orange.

2D-OPG TAU-n area   3D-DVT Hounsfield   display TAU-n Average(log)
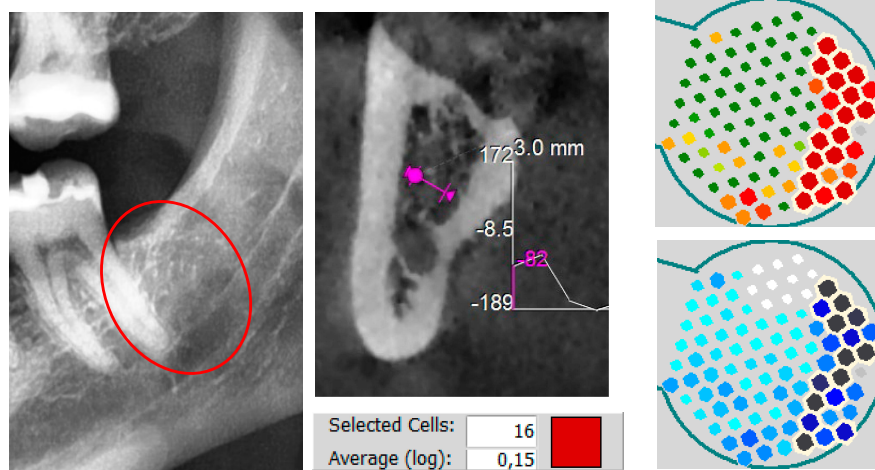
Figure 3 The top right picture shows a clear division into two parts: The right part, which points distally when the TAU sensor is inserted, corresponds with the strong red coloration to a high attenuation and thus reduced bone density with possible osteolysis. The clear distinction from red to green shows that the distal root of tooth 37 was detected in the mesial part of the sensor. In TAU-n, hard substance with low attenuation is marked with green or light-blue to white. The sensor fields marked white-blue to black in the lower right image allow an even more detailed interpretation of the attenuation. Both TAU-n measurement images correspond with the HU value of −8.5 in the edentulous are of 38 shown in the center part of Figure 3.

2D-OPG TAU-n area   3D-DVT Hounsfield   display TAU-n Average(log)

Figure 4 Reduced bone density in HU and TAU-n in the maxillary area 28 corresponding to the area of BMD/AIOJ/FDOJ.
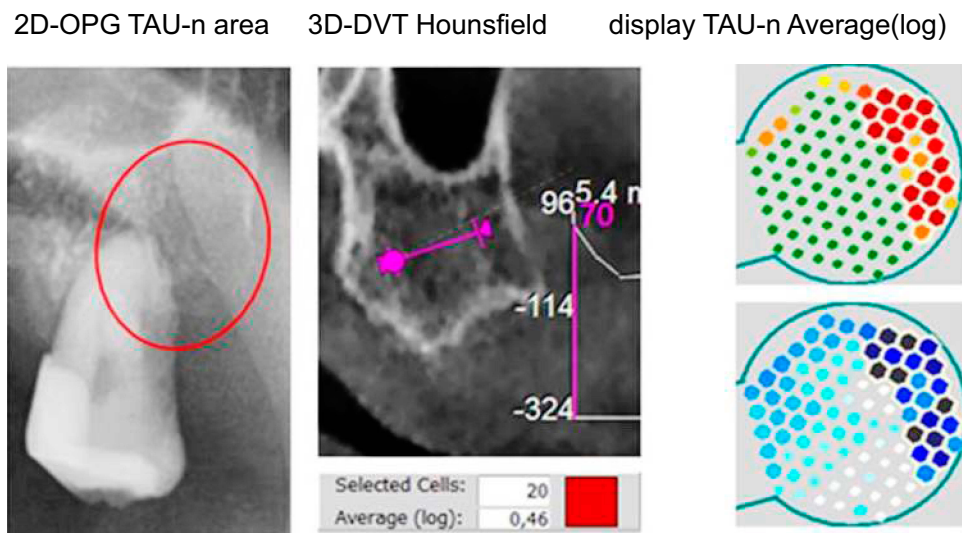
2D-OPG TAU-n area 3D-DVT Hounsfield   display TAU-n Average(log)
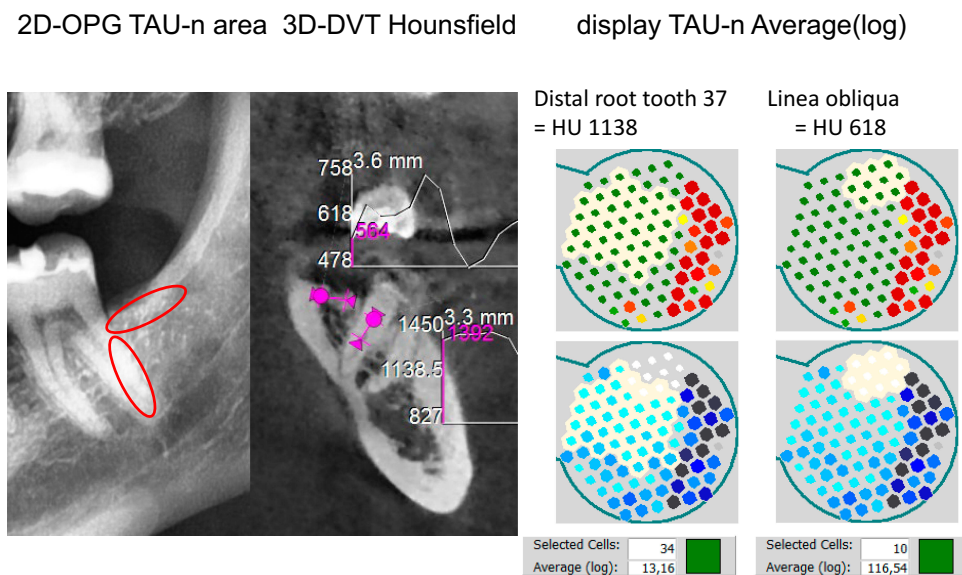

Figure 5 Two areas of increased density: The distal root of tooth 37 and the cortical density of oblique line as the upper rim of area 38. The left image marks the two measuring areas with red circles and with HU values of +1138 for the root portion and +618 for the oblique line. Average(log) of these two very radiopaque areas are in TAU-n 13 and 116 and thus in green.

Methods for Validation of TAU-n Measurements

How reliable are these measurements? To answer this question, we compare four parameters. Two options for the pre-operative diagnosis of AIOJ/BMD/FDOJ:

1. Digital Volume Tomography (DVT)/CBCT (Cone beam computed tomography/CBCT) with the option of HU measurement.

2. Use of TAU-n as a novel radiation-free option for bone density measurement

Two options for post-op confirmation or failure of pre-operative 1) and 2):

3. Histology findings of operated jawbone samples.

4. Multiplex analysis of the RANTESS/CCL5 (R/C) expression of operated jawbone samples as proof or disprove of inflammation.

Two-Dimensional X-Ray with Orthopantomogram

Since the occurrence and phenomena of AIOJ, FDOJ and BMD are practically undetectable in any type of X-ray

examination, they are largely unknown, widely controversial or even disputed.[10] The existence of BMD/AIOJ/ FDOJ has been predominantly ignored in mainstream dentistry. The reason is that conventional two-dimensional X-ray techniques with orthopantomograms (OPG) are only able to visualize areas affected by BMD/AIOJ/ FDOJ to a limited extent.[11] 2D-OPG is then useful when there is a mix of osteolysis and osteosclerosis apparent.[12] At the same time, a significant loss of bone mineral (30–50%) is required before it becomes visual on the OPG.[13,14] In view of these diagnostic difficulties, BMD/AIOJ/FDOJ is often underdiagnosed by dentists.[14] In 2D-OPG pathological changes can be completely absent without pathognomonic radiological findings pointing to AIOJ/BMD/ FDOJ. The same applies to the reduced mineralization of BMD/AIOJ/FDOJ.[15] Even months after tooth removal or spontaneous tooth loss, the cortical walls of the alveoli remain intact without showing progressive destruction due to progressive osteolysis.[16] Consequently, we did not integrate the use of 2D-OPG in the pre-operative diagnosis of BMD/AIOJ/FDOJ.

Three-Dimensional X-Ray with Digital Volume Tomography

Modern X-ray methods like DVT/CBCT allow the clinician to perform a three-dimensional assessment of the jawbone with the determination of X-ray attenuation coefficients expressed in Hounsfield units (HU).[17,18] SimPlant software bone density measurements performed in the posterior mandible (3D Diagnostix, Boston, MA, USA) showed a mean CT value of 669.6 HU.[19] Further investigations classified the cancellous bone density of the jaw bone into five categories, with the worst bone density for a normal jaw bone being <150 HU (Class 5). Therefore, the HU values generated in our study (range: <150 to −370) show osteolysis of the jawbone for Class 5 cases.[20] The device used by our team for DVT diagnosis was an orange 3D PaX-i3D Duo Multi X-ray, which displays HU values over a freely selectable jaw distance. In X-ray technology, the HU scale is generally scientifically recognized for assessing bone density.[17–20] The values are assigned to physical states and tissues. The HU scale starts at −1000 for the damping coefficient of air, for fat it is –120, for healthy cancellous bone at +300 to +400 and for cortical bone at +1800 to over +2000. By definition the HU for water = 0.

For HU measurement we have a DVT from Orangedental PaX-i3D Duo 3D Multi X-ray unit 3D with corresponding software for evaluation of HU at our disposal. In accordance with DIN 6868–57, the availability of the viewing monitors with a contrast of >40:1, a brightness of at least 120 cd/m2 and a DICOM characteristic was maintained. Our device displays the mean value of an optically freely selected measurement path with the maximum and minimum values as a curve (see Figures 3, 4 and 5).

Bone Density Comparison: Hounsfield Units versus TAU-n

Example 1: Measuring Reduced Bone Density with HU and TAU-n in Mandible

Figure 3 shows in the left picture the TAU-n measuring range of area 38 with inconspicuous X-ray structure in 2D-OPG; the picture in the center shows in cross-section the DVT at this point with the HU attenuation coefficient at a level of −8.5. According to the HU scale, the HU attenuation coefficient is below that of water (= 0 HU). Thus, a reduced bone density in this area can be concluded with suspicion of osteolysis (AIOJ/BMD//FDOJ).

Example 2: Measurement of Reduced Bone Density with DVT/HU and TAU-n in the Maxilla

Figure 4 shows a HU value of −114 in the retromolar area 19 and thus reduced bone density. As shown in Figure 4, the distal part of the root tooth 28 is also visible here with contrasting green and white-light blue staining in TAU-n. The toothless alveolar ridge disto-cranial of tooth 28 shows the strongly reduced bone density with intensive red and blue-black colouring, presumably osteolysis/osteonecrosis of jawbone. HU and TAU-n attenuation coefficients fully correspond with each other.

Example: Measuring High Bone Density with DVT/HU and TAU-n

Show examples of TAU-n measurements with maximum attenuation. compares ranges of minimum attenuation in HU and TAU-n and the corresponding attenuation coefficients. For this purpose, the sensor elements are marked which show green colors in TAU-n (top right) or white/ light blue (bottom right). In the bottom center, the logarithmic mean value of the measurement of the "best" sensor elements (= minimum attenuation) is displayed (Average(log)).

Figure 5 (left 2D-OPG) shows two areas of increased bone density: the distal root of tooth 37 and the cortical density of the oblique line on the cranial rim of area 38.

The red circles mark the two measuring areas with HU values of 1138 for the root portion and 618 for the oblique line (3D-DVT). The corresponding measuring points in TAU-n are marked (right part of Figure 5) and output is shown as logarithmic average values. The HU of 1138 corresponds to the TAU-n value of 13.16 and the HU of 618 corresponds to a TAU-n value of 116.54.

Comparison: TAU-n Vs Histology of BMD/FDOJ

Each BMD/AIOJ/FDOJ sample was histologically examined (1). Almost all showed the following typical finding:

> Chronic degenerative changes mix with non-reactive adipocyte necrosis. The amount of fat cells is significantly increased. There are no typical signs of inflammation, in particular no inflammatory cell reaction. The fatty-degenerative and osteolytic aspect predominates due to an insufficient metabolic supply (trophic disorder). Bone marrow shows enlarged intertrabecular spaces, often small necrotic bone fragments, fatty micro-vesicles and pools of liquefied fat similar to oil cysts. Small nerve fibers are a prominent feature of most BMD/AIOJ/FDOJ fibroses.

Based on the results of several hundred histological BMD/AIOJ/FDOJ samples, we defined five different characteristics to build up statistics: "FDOJ" (how far does pathology confirm the presence of FDOJ), "fibrosis", "necrotic adipocytes", "trophic disorder" and "no inflammatory cells". For evaluation purposes, we defined these five terms and assigned them to a number from 0 to 4, depending on their strength or presence. Regarding the histological results, if none of these five characteristics in total would give a value of "0" in grading intensity, this would indicate that the preoperative diagnosis of BMD/AIOJ/FDOJ in this jaw area was proven wrong. At the end of the evaluation (see Chapter 7 Results) the grading intensity is the sum of the individual evaluations of FDOJ, fibrosis, necrosis, trophic disorder and inflammatory cells. The higher the grading intensity values (maximum = 20), the more reliable was the preoperative evaluation by DVT and TAU-n. Values <4 correspond to a misdiagnosis under histological criteria.

(1 Institute for Pathology & Cytology Dr. Zwicknagel/ Assmus (Freising, Germany))

Comparison: TAU-n in Fatty-Degenerative Osteolysis (in Jawbone with Reduced Bone Density) versus Local RANTES/CCL5 Overexpression

Morphology of BMD/AIOJ/FDOJ and Local RANTES/CCL5 Expression

What does BMD/AIOJ/FDOJ look like clinically? The histologically defined main components of BMD/AIOJ/FDOJ are necrotic adipocytes (Figure 6)

The authors examined in detail the tissue in such jaw lesions that appears as fatty lumps inside an intact cortical bone.[6,7] They showed that the fatty lumps found are biochemically extremely active and produce certain cytokines in large quantities, in particular the chemokine RANTES/CCL-5 (R/C). The expression levels of these cytokines are also elevated in a number of systemic diseases such as cancer, dementia, multiple sclerosis or arthritis. There is strong evidence that the development and persistence of a variety of systemic diseases may be associated with R/C overexpression by BMD/AIOJ/FDOJ. However, in most of these cases, the local effect of neuralgic pain is missing.[6,7,21,22] It has also been plausibly shown that AIOJ/BMD/FDOJ describes the pathological condition of the jawbone, which is listed in code M87.0 of the ICD-10 (International Code of Diseases, Tenth Revision (ICD-10)).

Comparison in FDOJ: DVT/HU Vs RANTES/CCL5 Expression

Figure 7 on the right shows the typical fatty-degenerative morphology of a BMD/AIOJ/FDOJ sample. Which clinical parameters correspond with this reduced HU- and TAU-n bone density values of this area? In addition to the histological findings, we can determine the R/C expression of the BMD/
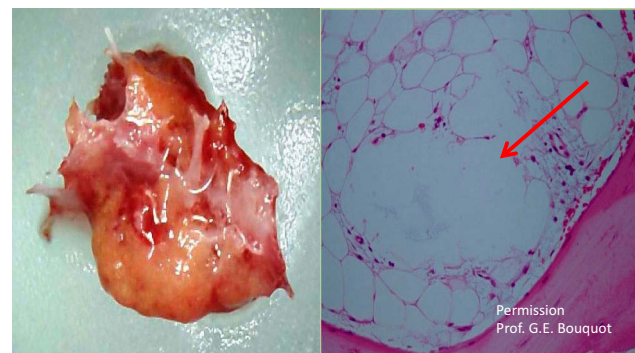

Figure 6 Left picture: Preparation of intraoperatively removed fatty-degenerative osteonecrosis from BMD/AIOJ/FDOJ; Right picture: Necrotic adipocytes confluent to so-called "oil cysts" with high-fat content (arrow points to such a big "oil cyst").
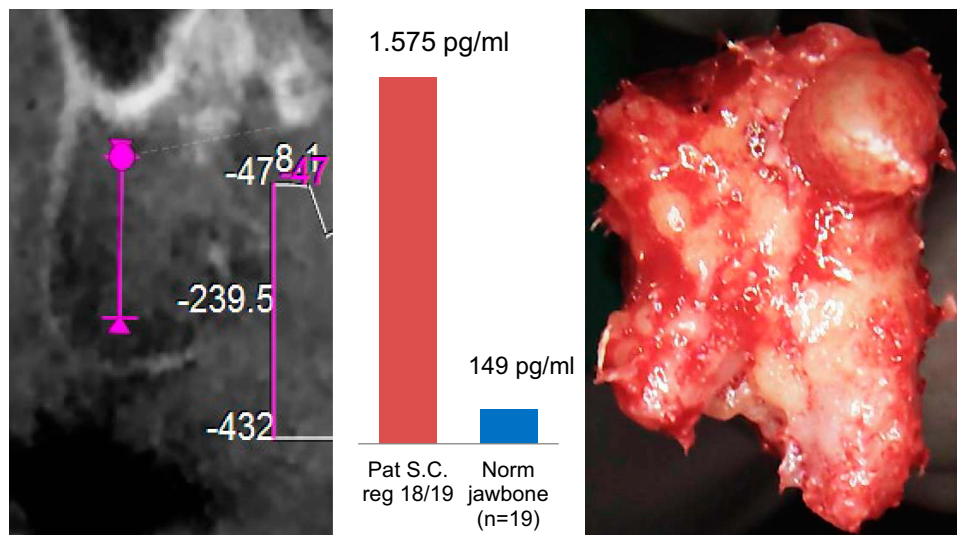
Figure 7 Left image shows DVT/HU of the retromolar area 18/19 with −239,5 Center image shows the R/C expression of the intraoperatively taken bone sample, which is about ten-fold higher than healthy jawbone. Thus, a chronic inflammatory process in the area of 18/19 has been confirmed by multiplex laboratory analysis. Right picture shows the fatty-degenerated cancellous bone from area 18/19, which structurally corresponds to the HU attenuation coefficient of −239. Related histologic findings in area 18/19 are: internal medullary spaces with myxoid or fibrillar degeneration of fatty tissue; trophic disorders.

AIOJ/FDOJ samples postoperatively. The example of BMD/AIOJ/FDOJ in Figure 7 compares the preoperatively determined HU values of a right upper wisdom tooth area with the fatty-degenerated cancellous bone, the postoperative histological findings and the multiplex analysis of the local R/C expression. The relationship between reduced medullary bone density, BMD/AIOJ/FDOJ and R/C overexpression with detection of R/C expression was discussed by the authors in previous publications.[6,7,21,22] Figure 7 deliberately omits the corresponding 2D-OPG.[9] In accordance with earlier publications,[6,7,21,22] this example demonstrates the morphology, the elevated R/C level (= red column; healthy jawbone shows 149.9 pg/mL R/C= blue column) and histology of the suitability of HU attenuation coefficients to assess BMD/AIOJ/FDOJ.

Summary of the Pre- and Post-Operative Presentation of an FDOJ

In summary, we use preoperative and postoperative diagnostic means in a BMD/AIOJ/FDOJ area for comparison: preoperative DVT/HU and bone density measurement with TAU-n. Postoperatively, histology examines fibrillary and fatty degeneration without inflammatory signs[25] and multiplex analysis shows the extent of R/C expression.

Results

Table 1A and B show the results of the preoperative determination of DVT/HU and TAU-n attenuation coefficients as "CavLog" numbers and postoperatively the R/C expression in pg/mL as well as the histological findings, presented numerically as "gradings" in 82 BMD/AIOJ/FDOJ cases.

Discussion

The presented study is patient-centered. Samples and data of all 82 patients are taken directly from day-today practice (2). The data were collected as part of the normal everyday medical care of the patients and evaluated retrospectively. In the context of clinically necessary surgical treatment of AIOJ/BMD/FDOJ, we examined removed BMD/AIOJ/FDOJ samples postoperatively histologically and for the content of R/C inflammatory messengers. The medical indication for BMD/AIOJ/FDOJ surgery in these patients was given by 2D-OPG and additional DVT/CBCT to determine bone density radiographically. This indication was supplemented by the measurement of bone density using TAU-n. The average age of the investigated group was 56.4 in a gender ratio of 59w/23m. The clinical case studies presented herein were performed as part of a case–control study and were deemed to be retrospective in nature. Approval was granted by IMD-Berlin forensic accredited Institute DIN EN 15189/DIN EN 17025. All patients provided their written informed consent (as outlined in the PLOS consent form) to participate in the studies,

(2 Clinic for Integrative Dentistry Gruenwalder Str. 10A 81547 Munich)

Table 1 The Results of the Preoperative Determination of DVT/HU and TAU-n Attenuation Coefficients

A									
Nr	**RANTES**	**HU**	**CavLg**	**FDOJ**	**Fibr**	**Necr**	**TroDi**	**Infla**	**Grad**
1	1.787.50	−211.0	0.32	2	2	3	2	0	9
2	9.899.32	−299.0	0.86	1	4	4	0	0	9
3	776.25	−328.0	0.21	3	0	0	1	1	5
4	820.00	−221.0	1.81	4	2	0	3	1	10
5	3.937.50	−230.0	0.42	4	3	0	0	0	7
6	1.987.50	−344.0	0.47	3	3	3	3	0	12
7	123.75	−293.0	1.18	3	4	2	2	0	11
8	5.700.00	−533.0	0.42	3	3	0	4	0	10
9	933.75	−290.0	3.18	3	1	3	3	0	10
10	706.25	−447.0	0.19	2	4	4	3	1	14
11	1.750.00	−390.0	0.82	4	4	4	3	0	15
12	775.00	−201.0	4.25	3	4	4	2	0	13
13	5.712.50	−350.0	0.80	4	4	2	3	1	14
14	4.325.00	−201.0	3.54	4	2	4	2	0	12
15	3.762.50	−291.0	0.37	2	4	4	4	1	15
16	1.825.00	−263.0	0.72	4	4	3	4	0	15
17	992.50	−340.0	0.41	4	4	4	0	0	12
18	557.50	−304.0	2.08	3	2	2	2	0	9
19	2.825.00	−431.0	0.71	3	2	2	3	0	10
20	873.75	−359.0	0.55	3	0	0	1	0	4
21	2.050.00	−280.0	0.23	3	3	0	0	2	8
22	5.412.50	−287.0	4.25	3	2	3	1	0	9
23	722.50	−345.0	1.25	2	3	0	0	2	7
24	3.250.00	−326.0	2.04	2	0	4	1	1	8
25	2.850.00	−250.0	0.21	0	0	0	0	0	0
26	3.162.50	−327.0	1.84	2	1	4	3	0	10
27	2.187.50	−93.0	0.47	3	2	2	2	0	9
28	902.50	−346.0	3.95	4	4	4	1	0	13
29	8.212.50	−298.0	1.06	4	3	2	3	0	12
30	1.675.00	−400.0	1.19	3	4	4	0	0	11
31	865.00	−502.0	0.53	4	4	0	3	0	11
32	767.50	−471.0	0.26	3	3	0	0	0	6
33	2.262.50	−334.0	1.22	3	1	3	2	0	9
34	1.400.00	−208.0	2.06	0	3	2	2	1	8
35	1.875.00	−200.0	0.77	2	4	0	2	0	8
36	1.575.00	518.0	0.65	4	4	3	4	0	15
37	9.998.15	−268.0	0.85	2	1	4	0	0	7
38	1.400.00	−213.0	0.74	4	1	4	4	0	13
39	495.00	−333.0	1.12	3	4	4	4	0	15
40	2.737.50	−379.0	1.21	4	1	4	4	0	13
41	3.725.00	−335.0	0.87	0	0	0	0	0	0
42	1.712.50	−235.0	0.69	4	4	1	4	0	13

B									
Nr	**RANTES**	**HU**	**CavLg**	**FDOJ**	**Fibr**	**Necr**	**TroDi**	**Infla**	**Grad**
43	2.962.50	−452.0	1.12	4	3	3	3	0	13
44	9.965.88	−322.0	0.54	4	1	4	0	0	9
45	5.362.50	−418.0	0.51	4	1	4	4	0	13
46	2.100.00	−301.0	0.33	4	3	3	3	0	13

(Continued)

Table 1 (Continued).

B									
Nr	RANTES	HU	CavLg	FDOJ	Fibr	Necr	TroDi	Infla	Grad
47	4.562.50	−186.0	1.59	4	3	4	3	0	14
48	2.425.00	−349.0	1.70	4	4	4	1	0	13
49	702.50	−376.0	0.15	4	2	2	4	2	14
50	2.425.00	−228.0	0.20	3	1	4	2	0	10
51	3.950.00	−261.0	0.30	4	4	4	4	1	17
52	2.000.00	−463.0	0.57	2	4	0	0	0	6
53	1.612.50	−345.0	0.71	4	3	4	3	0	14
54	527.50	−438.0	0.29	3	1	4	0	1	9
55	1.275.00	−363.0	1.06	0	0	0	0	0	0
56	1.700.00	−432.0	0.76	4	2	4	3	1	14
57	1.587.50	−198.0	0.51	4	2	4	3	0	13
58	486.25	−260.0	0.47	4	1	4	1	0	10
59	518.75	−294.0	0.90	4	1	3	4	0	12
60	1.337.50	−373.0	0.47	3	4	1	2	0	10
61	2.112.50	−249.0	0.50	4	4	0	4	0	12
62	810.00	−243.0	0.41	4	3	3	3	0	13
63	1.078.75	−440.0	0.60	4	4	4	3	0	15
65	863.75	−227.0	0.81	0	0	0	0	0	0
67	405.00	−450.0	1.11	4	3	4	1	2	14
68	2.875.00	−387.0	0.26	4	1	4	0	0	9
70	1.800.00	−308.0	0.41	1	4	0	0	0	5
72	1.337.50	−248.0	1.77	1	4	0	0	0	5
73	6.512.50	−348.0	0.23	4	2	3	3	0	12
74	893.75	−264.0	2.73	3	4	4	3	0	14
75	1.775.00	−168.0	1.58	4	2	4	3	0	13
76	146.25	−265.0	0.20	2	3	1	0	0	6
77	8.062.50	−373.0	1.02	3	1	2	3	0	9
80	1.875.00	−173.0	1.95	4	2	3	3	0	12
81	910.00	−454.0	0.77	0	0	0	0	0	0
82	645.00	−189.0	2.29	3	3	1	0	1	8
MV	2.459.37	−303.7	0.9	3.01	3	2.4	1.99	0.3	10.2

Notes: Table 1 a and Table 1 b: Nr = number of patient in 82 BMD/AIOJ/FDOJ cases; RANTES = multiplex value of RANTES/CCL5 expression in pg/mL of jawbone sample; HU = Hounsfield units of CBCT of corresponding area of jawbone surgery, CavLg = TAU-n value; FDOJ = fatty-degenerative osteonecrosis of jawbone in histological findings from 0 to 4 in intensity or obvious presence; Fibr = presence of fibrosis; Necr = presence of necrosis; TroDi = presence of a trophic disorder; Inflam = no inflammatory cells are present; Grade = sum of five upper characteristics as grading intensity. Samples marked in yellow and graded in 0 show no histological evidence for BMD/AIOJ/FDOJ.

Discussion of the Hounsfield Units

With a mean value of –303 HU, the BMD/AIOJ/FDOJ sites diagnosed with DVT/HU are clearly below the minimum value for healthy jawbone of +300 HU.[23,24] The bone density is therefore clearly below normal.

Discussion of the TAU-n Average(Log) Values

The limit value of TAU-n Average(log) is 100: high-density areas (average[log] ≥100) are indicated in TAU-n by the color green and low-density areas by red (average[log] <100). With the mean value of 0.9 [log], the areas examined with TAU-n are preoperatively well within the display range red of BMD/AIOJ/FDOJ typical reduction of bone density.

Discussion of Histology

From 82 histological findings, five parameters were defined for the evaluation of a BMD/AIOJ/FDOJ. Depending on intensity or obvious presence, a number from 0 to 4 was assigned to the finding. Table reading:

a) "FDOJ": Pathology confirms the presence of BMD/ AIOJ/FDOJ. The mean value of 3.01 in Table 1A and B confirms on average the presence of BMD/ AIOJ/FDOJ in almost all 82 BMD/AIOJ/FDOJ samples.

b) "Fibr": presence of fibrosis. The mean value of 2.47 confirms fibrosis in all BMD/AIOJ/FDOJ samples.

c) "Necr": presence of necrosis. The mean value of 2434 confirms on average the necrosis of the adipocytes in the 82 BMD/AIOJ/FDOJ samples.

d) "TroDi": presence of a trophic disorder. The mean value of 2 confirms on average the trophic disturbances in the 82 BMD/AIOJ/FDOJ samples.

e) "Inflam": No inflammatory cells are present (free from acute inflammatory reactions). The mean value of 0.25 confirms on average the absence of inflammatory cells in the 82 BMD/AIOJ/FDOJ samples.

f) "Grade": sum of these five characteristics as "grading intensity". The mean value of 10.2 confirms on average the presence of a histologically defined BMD/AIOJ/ FDOJ in the 82 BMD/AIOJ/FDOJ samples.

Nevertheless, there are five samples (marked yellow in Table 1and b and consistently graded in 0) in which the pathologist cannot find histological evidence for BMD/AIOJ/ FDOJ. A contradiction of these negative histological findings is shown.

a) To the positive results of BMD/AIOJ/FDOJ in these five cases with overexpressed R/C of 2.850, 3.725, 1.275, 863 and 910 pg/mL, respectively, at a normal healthy bone value of 149.90 pg/mL.

b) To the positive results of BMD/AIOJ/FDOJ in these five cases, each with strongly negative HUs with −250.0, −335.0, −363.0, −227.0 and −454.0 at a standard value of >300.

c) On the positive findings of BMD/AIOJ/FDOJ in these five cases with very low Cav [log] values of 0.21, 0.87, 1.06, 0.81 and 0.77 with a healthy limit of >100.

Therefore, it can be concluded that the BMD/AIOJ/ FDOJ findings were correct preoperatively by DVT/HU and TAU-n. However, the light microscopically histology performed postoperatively shows the highest failure rate, whilst all R/C expression values proved the existence of BMD/AIOJ/FDOJ.

Discussion of the RANTES/CCL5 Expression

The normal range of R/C expression in the healthy jawbone is 149 pg/mL In our cohort of 82 patients, the mean value of 2459.37 pg/mL is approximately 15 times higher than in healthy bone marrow areas and thus confirms the preoperative TAU-n values postoperatively.

Summary

In summary, all four evaluation criteria predominantly confirm the presence of BMD/AIOJ/FDOJ in each of the 82 samples. Validation of the TAU-n method in comparison to the other methods was thereby confirmed. TAU-n fits seamlessly into the reliability of the other methods.

Conclusion

The data and procedures presented show that the TAU-n device provides reliable bone density data. Thus, it is a metrologically unbiased alternative to the increasingly critically assessed X-ray radiation[26,27] and the more stringent radiation protection laws.[28] This work is at the interface of morphology and immunology of chronic osteolytic changes in the jawbone. The presented medullary mineralization and ossification disorder of BMD/ AIOJ/FDOJ is not an isolated clinical picture as it is often presented in clinical research on osteoporosis or bisphosphonate-induced osteonecrosis. Rather, it is a chronic osteo-immunologically derailed condition that can be regarded as an additional stress factor in immune and inflammatory diseases. Its character of a "silent inflammation" with proinflammatory chemokine expression, especially of R/C, shows itself as a common stress factor or possibly even a common trigger of numerous immunological systemic diseases.[29,30] For their simple detection, the reliable, unstressed and easy-to-use TAU-n device is available.

Abbreviations

AIOJ, Aseptic-Ischemic Osteonecrosis of Jawbone; BMD, Bone Marrow Defects; CBCT, Cone Beam Computed Tomography; CCL5, Chemokine (C-C motif) ligand 5; DVT, Digital Volume Tomography; FDOJ, Fatty-Degenerative Osteonecrosis/Osteolysis of Jawbone; HU, Hounsfield Units; Log, logarithmic; OPG, Orthopantomogram; R/C, RANTES/ CCL5; RANTES, Regulated on Activation, Normal T cell Expressed and Secreted; TAU, Trans-Alveolar Ultrasonogra-

phy; TAU-n, New Trans-Alveolar Ultrasonography Device; US, Ultrasound.

Acknowledgments

Disclosure

CaviTAU® (Munich, Germany), the company that designed the new TAU-n apparatus and associated software, provided these tools without charge for the purposes of this study. The ultrasonography procedure was carried out at the Clinic for Integrative Dentistry Munich. CaviTAU® and the Clinic for Integrative Dentistry are in ongoing discussions regarding numerous collaborative arrangements to further improve and verify the new TAU apparatus, CaviTAU®, as it is introduced to the market. Dr. Johann Lechner is the holder of a patent PCT/EP2018/084199 used in CaviTAU®. The authors report no other conflicts of interest in this work.

References

1. Patini R, Gallenzi P, Lione R, Cozza P, Cordaro M, et al. Ultrasonographic evaluation of the effects of orthodontic or functional orthopaedic treatment on masseter muscles: a systematic review and meta-analysis. *Medicina*. 2019;55(6):256.
2. Lipani CS, Natiella JR, Greene GW Jr. The hematopoietic defect of the jaws: a report of sixteen cases. *J Oral Pathol*. 1982;11(6):411–416. doi:10.1111/j.1600-0714.1982.tb00184.x
3. Lee S-C, Jeong CH, Im HY, et al. Displacement of dental implants into the focal osteoporotic bone marrow defect: a report of three cases. *J Korean Assoc Oral Maxillofacial Surgeons*. 2013;2(94):39.
4. Bouquot JE, Roberts AM, Person P, Christian J. Neuralgia-inducing cavitational osteonecrosis (NICO). Osteomyelitis in 224 jawbone samples from patients with facial neuralgia. *Oral Surg Oral Med Oral Pathol*. 1992;73(3):307–319. doi:10.1016/0030-4220(92)90127-C
5. Bouquot J, Martin W, Wrobleski G. Computer-based thru-transmission sonography (CTS) imaging of ischemic osteonecrosis of the jaws – a preliminary investigation of 6 cadaver jaws and 15 pain patients. *Oral Surg Oral Med Oral Pathol Oral Radiol Endod*. 2001;92:550.
6. Lechner J, von Baehr V. RANTES and fibroblast growth factor 2 in jawbone cavitations: triggers for systemic disease? *Int J Gen Med*. 2013;6:277–290. doi:10.2147/IJGM.S43852
7. Lechner J, Schuett S, von Baehr V. Aseptic-avascular osteonecrosis: local `silent inflammation` in the jawbone and RANTES/CCL5 overexpression. *Clin Cosmet Investig Dent*. 2017;9:99–109. doi:10.2147/CCIDE.S149545
8. Al-Nawas B, Grotz KA, Kann P. Ultrasound transmission velocity of the irradiated jaw bone in vivo. *Clin Oral Invest*. 2001;5(4):266–268. doi:10.1007/s00784-001-0133-4
9. Klein MO, Grotz KA, Manefeld B, Kann PH, Al-Nawas B. Ultrasound transmission velocity for non-invasive evaluation of jaw bone quality in vivo prior to dental implantation. *Ultrasound Med Biol*. 2008;34 (12):1966–1971. doi:10.1016/j.ultrasmedbio.2008.04.016
10. Lechner J. Validation of dental X-ray by cytokine RANTES - comparison of X-ray findings with cytokine overexpression in jawbone. *Clin Cosmet Investig Dent*. 2014;6:71–79. doi:10.2147/CCIDE.S69807
11. Wells PNT. Ultrasonic imaging of the human body. *Rep Prog Phys*. 1999;62(5):676. doi:10.1088/0034-4885/62/5/201
12. Njeh C, Hans D, Fuerst C, Gluer C, Genant HK. *Quantitative Ultrasound. Assessment of Osteoporosis and Bone Status*. United Kingdom: Martin Dunitz. Ltd; 1999.
13. Chiandussi S, Biasotto M, Dore F, Cavalli F, Cova M, Lenarda R. Clinical and diagnostic imaging of bisphosphonate- associated osteonecrosis of the jaws. *Dentomaxillofac Radiol*. 2006;35(4):236–243. doi:10.1259/dmfr/27458726
14. Store G, Boysen M. Mandibular osteoradionecrosis: clinical behaviour and diagnostic aspects. *Clin Otolaryngol*. 2000;25(5):378–384. doi:10.1046/j.1365-2273.2000.00367.x
15. Stockmann P, Hinkmann FM, Lell MM, et al. Panoramic radiograph computed tomography or magnetic resonance imaging. Which imaging technique should be preferred in bisphosphonate-associated osteonecrosis of the jaw? A prospective clinical study. *ClinOralInvestig*. 2010;14(3):311–317.
16. Grötz KA, Al-Nawas B. Persisting alveolar sockets–a radiologic symptom of BP-ONJ? *J Oral Maxillofac Surg*. 2006;64(10):1571–1572. doi:10.1016/j.joms.2006.05.041
17. Swennen GR, Schutyser F. Three-dimensional cephalometry: spiral multi-slice vs cone-beam computed tomography. *Am J Orthodontics Dentofacial Orthopedics*. 2006;130(3):410–416. doi:10.1016/j.ajodo.2005.11.035
18. Mah P, Reeves TE, McDavid WD. Deriving Hounsfield units using grey levels in cone beam computed tomography. *Dentomaxillofacial Radiol*. 2010;39(6):323–335. doi:10.1259/dmfr/19603304
19. Norton MR, Gamble C. Bone classification: an objective scale of bone density using the computerized tomography scan. *Clin Oral Implants Res*. 2001;12(1):79–84. doi:10.1034/j.1600-0501.2001.012001079.x
20. Misch CE. Bone density: a key determinant for clinical success. In: Misch CE, editor. *Contemporary Implant Dentistry*. 2nd ed. St Louis: CV Mosby Company; 1999:109–118.
21. Lechner J, von Baehr V. Hyperactivated signaling pathways of chemokine RANTES/CCL5 in osteopathies of jawbone in breast cancer patients—case report and research. *Breast Cancer*. 2014;8:89–96. doi:10.4137/BCBCR.S15119
22. Lechner J, Rudi T, von Baehr V. Osteoimmunology of tumor necrosis factor-alpha, IL-6, and RANTES/CCL5: a review of known and poorly understood inflammatory patterns in osteonecrosis. *Clin Cosmet Investig Dent*. 2018;10:251–262. doi:10.2147/CCIDE.S184498
23. Ganz SD. Conventional CT and cone beam CT for improved dental diagnostics and implant planning. *Dent Implantol Update*. 2005;16 (12):89–95.
24. Lee S, Gantes B, Riggs M, Crigger M. Bone density assessments of dental implant sites: 3. Bone quality evaluation during osteotomy and implant placement. *Int J Oral Maxillofac Implants*. 2007;22(2):208–212.
25. Lechner J, Noumbissi S, von Baehr V. Titanium implants and silent inflammation in jawbone – a critical interplay of dissolved titanium particles and cytokines TNF-a and RANTES/CCL5 on overall health? *EPMA J*. 2018;9(3):331–343. doi:10.1007/s13167-018-0138-6
26. Brenner DJ, Elliston CD, Hall EJ, Berdon WE. Estimated risks of radiation induced fatal cancer from pediatric CT. *AJR*. 2001;176 (2):289–296. doi:10.2214/ajr.176.2.1760289
27. Vañó E, Miller DL, Martin CJ, et al.; ICRP- International Commission on Radiological Protection. Diagnostic reference levels in medical imaging. ICRP Publication 135. *Ann ICRP*. 2017;46(1):1–144. doi:10.1177/0146645317717209

28. Strahlenschutzgesetz (StrlSchG) Artikel 1 G. v. 27.06.2017 BGBl. I S. 1966; Strahlenschutzverordnung (StrlSchV) Artikel 1 V. v. 29.11.2018BGBl. I S. 2034, 2036; Gesetz zur Neuordnung des Rechts zum Schutz vor der schädlichen Wirkung ionisierender Strahlung (StrlSchGEG) G. v. 27. 06.2017BGBl. I S. 1966.

29. von Luettichau I, NELSON P, PATTISON J, et al. RANTES chemokine expression in diseased and normal human tissues. *Cytokine*. 1996;8(1):89–98. doi:10.1006/cyto.1996.0012

30. Tsukishiro S, Suzumori N, Nishikawa H, Arakawa A, Suzumori K. Elevated serum RANTES levels in patients with ovarian cancer correlate with the extent of the disorder. *Gynecol Oncol*. 2006;102(3):542–545. doi:10.1016/j.ygyno.2006.01.029